



LAWRENCE
LIVERMORE
NATIONAL
LABORATORY

Our contribution to the Faraday Discussion on Gold

A. Wittstock, A. Wichmann, J. Biener, M. Baumer

June 14, 2011

Faraday Discussion 152
Cardiff, United Kingdom
July 4, 2011 through July 6, 2011

Disclaimer

This document was prepared as an account of work sponsored by an agency of the United States government. Neither the United States government nor Lawrence Livermore National Security, LLC, nor any of their employees makes any warranty, expressed or implied, or assumes any legal liability or responsibility for the accuracy, completeness, or usefulness of any information, apparatus, product, or process disclosed, or represents that its use would not infringe privately owned rights. Reference herein to any specific commercial product, process, or service by trade name, trademark, manufacturer, or otherwise does not necessarily constitute or imply its endorsement, recommendation, or favoring by the United States government or Lawrence Livermore National Security, LLC. The views and opinions of authors expressed herein do not necessarily state or reflect those of the United States government or Lawrence Livermore National Security, LLC, and shall not be used for advertising or product endorsement purposes.

Nanoporous gold: a new gold catalyst with tunable properties

Arne Wittstock,^{1,2*} Andre Wichmann¹, Jürgen Biener², and Marcus Bäumer¹

¹ Institute of Applied and Physical Chemistry, University Bremen, Leobener Str. NW2, 28359 Bremen, Germany

² Nanoscale Synthesis and Characterization Laboratory, Lawrence Livermore National Laboratory, Livermore, California, USA

* Corresponding author: awittstock@uni-bremen.de

Abstract

10 Nanoporous gold (np-Au) represents a novel nanostructured bulk material with very interesting perspectives in heterogeneous catalysis. Its monolithic porous structure and the absence of a support or other stabilizing agents opens up unprecedented possibilities to tune structure and surface chemistry in order to adapt the material to specific catalytic applications. We investigated three of these tuning options in more detail: change of the porosity by annealing, increase of activity by the deposition of oxides and change of activity and selectivity by bimetallic effects. As an example for the latter case, the effect of Ag impurities will be discussed. The presence and concentration of Ag can be correlated to the availability of active oxygen. While for the oxidation of CO the activity of the catalyst can be significantly enhanced when increasing the content of Ag, we show for the oxidation of methanol that the selectivity is shifted from partial to total oxidation. In a second set of
20 experiments, two different metal-oxides were deposited on np-Au, praseodymia and titania. In both cases, the surface chemistry changed significantly. The activity of the catalyst for oxidation of CO was increased by up to one order of magnitude after modification. Finally, we used adsorbate controlled coarsening to tune the structure of np-Au. In this way, even gradients in the pore- and ligament size could be induced, taking advantage of mass transport phenomena.

Introduction

In recent years, there has been an increasing interest in monolithic nanoporous materials for various applications, such as for energy storage and conversion materials, sensors and actuator materials and catalysts.¹⁻⁴ Among various strategies to generate nanoporosity, the corrosion of alloys turned out to be especially suitable. In this context, nanoporous gold (np-Au), in particular, gained considerable
30 interest. The corrosion of a Au alloy containing at least one less noble constituent, such as Ag or Cu, results in a bulk nanostructured material consisting of almost pure gold.^{5, 6} The structure of the material is characterized by a three-dimensional porous network of ligaments in the range of typically some tens of nanometers (see Figure 1). Starting about ten years ago, an increasing number

of publications dealt with the preparation of the material and its promising applications e.g. as catalyst, sensor material, and high surface area electrode.^{4, 5, 7, 8} One key element for these applications is the open cell morphology of the material that provides a high surface area and makes it penetrable for gases and liquids. The chemical interaction of molecules with the surface, i.e., the surface chemistry can then even lead to an observable macroscopic response. When the material is, for example, exposed to an oxidizing agent, such as ozone, that roughly generates one monolayer of surface bonded oxygen, the material can be reversibly strained on a macroscopic scale by altering the surface stress state.⁹

The high surface area also renders np-Au interesting for catalytic applications. In 2006, Zielasek et al. and, in 2007, Ding et al. independently discovered that this gold material is a highly active catalyst for the oxidation of CO with molecular oxygen at temperatures as low as 0 °C.^{10, 11} This finding came as a bit of surprise, as the majority of active gold catalysts is typically comprised of gold nanoparticles in the range of only a few nanometers on a suitable oxide support, such as titania or ceria.¹²⁻¹⁵ Since the first reports of the unexpectedly high activity of gold-based catalysts in the 1980ies the interaction of gold and the support has been discussed to be a crucial factor for catalytic activity. Consequently, the origin of the catalytic activity of unsupported np-Au has been a matter of debate in the recent literature.

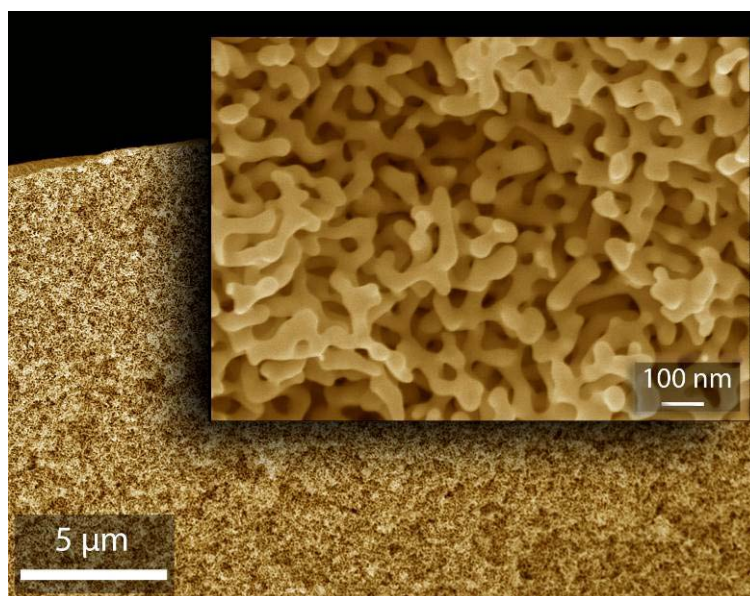


Figure 1: Scanning electron micrographs of a cross section of the np-Au material

In contrast to supported catalysts, only two factors can play a role. On the one hand, low coordinated gold atoms at steps and kinks - probably constituting a large part of the surface atoms - may be able to activate the molecular oxygen – the crucial step for gold based oxidation catalysts.¹⁶⁻¹⁸ On the

60 other hand, the material still contains traces of the less noble metal such as Ag – being the other constituent of the starting alloy - in the range of ~ 1 at%.¹⁹ If this second metal is enriched at the surface – in the case of Ag with surface concentration in the range of up to several atomic percent -, it can very well contribute to the catalytic activity.²⁰ In comparison to Au, molecular oxygen tends to bind more strongly to metals, such as Ag and Cu and thus is more easily activated.²¹ It was thus discussed to what extent this ad-metal contributes to the catalytic activity especially with respect to the activation of O₂.^{20, 22} Recently, also UHV model experiments and DFT calculations were employed to further understand this aspect of the surface chemistry of np-Au.²³

When dealing with catalysis, one has not only to consider the surface chemistry but also mass transport phenomena, which become particularly pronounced in case of materials with high porosity. In the case of np-Au the porous structure is very homogeneous with narrow ligament and pore size
70 distributions throughout the material. This well-defined structure provides a good starting point for quantifying mass transport phenomena in np-Au based on straightforward assumptions.²⁰ For example, the efficiency of a 200-micron-thick np-Au disk for CO oxidation is only about 10 % as the reaction of CO is faster than the mass transport limited supply from the outer gas phase leading to a fast decrease of the concentration within the material.²⁰ In order to find an optimum between low mass transport limitation (large pores) and high surface area (small pores), a controlled tuning of the ligament sizes is essential.

By using the intrinsic instability of nanostructures, one can induce coarsening of the ligaments by treatment at elevated temperatures.²⁴⁻²⁶ For np-Au, such a coarsening sets in at annealing temperatures above ~ 200 °C.^{27, 28} In this way, the ligament and pore sizes can be tailored within
80 several orders of magnitude, starting from ~ 5 nm up to microns.²⁹ Interestingly, the morphology of the material in terms of relative density and porosity stays constant, while the size of the ligaments and pores is increased. This behaviour is the result of curvature driven diffusion of surface atoms.^{25,}
²⁹ Accordingly, adsorbates, such as atomic oxygen, which are able to stabilize low coordinated Au surface atoms³⁰ do have an impact on the diffusion of surface atoms and thus on the coarsening during heat treatment of np-Au. When, for example, np-Au is annealed under an ozone containing atmosphere generating surface bonded oxygen, the size of the ligaments and pores of np-Au can be conserved, at least below the desorption temperature of oxygen on the gold surface (~ 500 K).^{25, 30}

In the present study, we describe different strategies to deliberately modify the properties of np-Au aiming at an optimization for specific applications with the emphasis on heterogeneous catalysis. On
90 the one hand, we will show that the surface chemistry of np-Au can be greatly changed by a second component, such as a metal or a metal-oxide. On the other hand, it will be demonstrated how the

feature size of np-Au and thus the mass transport properties within the pores can be tuned by adsorbate controlled coarsening.

100 Taking advantage of the fact that some residual Ag is still contained in the material after preparation, we systematically investigated the dependence of the activity and selectivity of two different oxidation reactions on the amount of residual Ag. We used CO and methanol oxidation as two different probe reactions, showing that a high amount of residual Ag can be beneficial for total oxidation reactions but a disadvantage in case of partial oxidations. We also investigated the effect of two different reducible oxides, praseodymia and titania, on the activity of oxidation reactions using molecular oxygen. Titania was chosen because of its widespread use for supported Au
nanoparticle catalysts and its possible use also in photo-catalysts.³¹ Praseodymia on the other hand was chosen because of its rich redoxchemistry and supposedly high lattice oxygen mobility.³² In both cases, we find a considerable increase of activity for CO oxidation of nearly one order of magnitude. We conclude that these changes are linked to the availability of active oxygen on the catalyst surface. Third, we used annealing under environmental control to investigate in more detail the influence of atomic oxygen on the stability of the np-Au structures, using ozone to generate surface bonded atomic oxygen.²⁵ The results reveal that the stability of the structures is strongly linked to the coverage by atomic oxygen. In combination with mass transport limited availability of ozone inside the pores, we can generate gradients in the porosity along the cross section of the np-Au
110 sample.

Materials and Methods

Disks of np-Au with a diameter of 5 mm and a thickness of 200 to 300 μm were prepared by corrosion of Ag(70at%)-Au(30at%) alloys in nitric acid. Two different methods were used: *free corrosion* where no external potential is applied and *galvanic corrosion* where the sample is held on a constant potential during the entire etching procedure. For *free corrosion*, the samples were placed on a glass frit in conc. nitric acid for 48 hours (HNO_3 , 65 wt%, Fluka Chemical Corp.). For *galvanic corrosion*, the sample was mounted in a typical three electrode setup. A 5 M solution of nitric acid was used as electrolyte (conc. HNO_3 diluted with ultra pure water ($> 18 \text{ M}\Omega$)). The potential was
120 held at 60 mV versus a platinum foil used as a reference electrode (Potentiostat, Wenking POS 88, BANK Electronics, counter electrode platinum foil). Samples containing different amounts of residual Ag were prepared by monitoring the current during etching and systematically varying the duration of corrosion, accordingly. For details see also ref. ³³.

For doping the np-Au samples with metal oxides two different methods were used. In case of titania, the samples were coated with a colloidal solution of titania particles. For this purpose, a sample of

np-Au was activated first and characterized in terms of catalytic activity for CO oxidation. A suspension of 2.5 g/L titania particles (Sigma-Aldrich, *nanopowder*, particles < 100 nm) in ethanol (Sigma Aldrich, p.A.) was prepared. For the sake of homogenisation and to generate a fine dispersion of particles, the suspension was sonicated for 30 minutes. Two droplets of the colloidal suspension were applied on each side of the np-Au disk. After ~ 1 minute the sample surface was rinsed with ethanol and eventually dried in nitrogen. In case of praseodymia, an impregnation and precipitation method was used. First, the np-Au sample was activated for CO oxidation. Afterwards, the sample was immersed in a solution of ethanol containing 20 g/L Pr(NO₃)₃ (Sigma-Aldrich, 99.9 %) for 15 minutes. After drying, the sample was heat treated (calcined) in air, starting at 60 °C and constantly heating up to 500 °C within 2 hours.

The catalytic experiments were performed using a continuous flow reactor especially designed for catalytic experiments with the np-Au disks (for details see also ref. ^{20, 33}). The feed gases were He (*Linde AG*, 5.0), O₂ (*Linde AG*, 4.5), and CO (*Linde AG*, 4.7). The total flow was always set to 50 sccm. The amount of methanol was controlled via its vapour pressure. First, a gas stream was saturated with methanol at room temperature (around 20 °C). Subsequently, the amount of methanol in the gas phase was adjusted by guiding the stream of saturated gas through a condenser. The stream of gases at the exit of the reactor was analyzed online by IR-Gas-Analyzers (URAS 3G, Hartmann und Braun) and GC-MS (100 µl sample pipe, Fison 8000 series (Column FS-innopeg-1000) coupled with a mass spectrometer TRIO 1000).

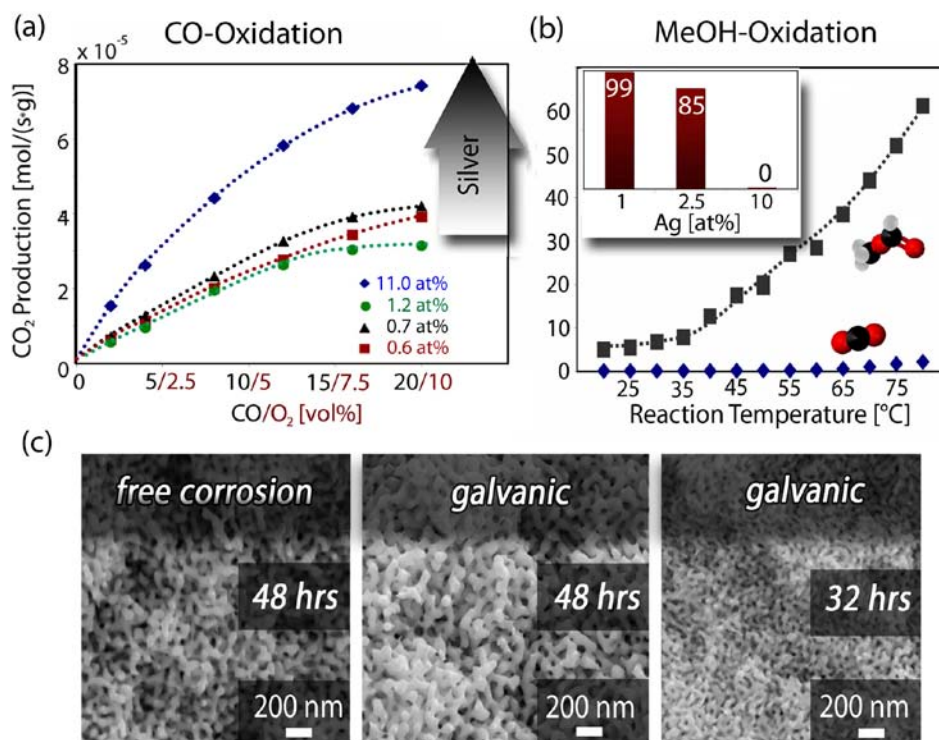
Annealing experiments with np-Au were carried out in a tube furnace under either an atmosphere of ultrapure He (5.0, *Linde AG*) or an ozone-oxygen mixture (~ 7vol% O₃ in 4.5 O₂, *Linde AG*) at a flowrate of 50 sccm (ozone generator type 802 N, ozone analyzer type 964, BMT Messtechnik Berlin). The coarsening of np-Au during annealing was analysed by cross-sectional scanning electron microscopy (XSEM). The average ligament diameter for each sample was then determined from ligament diameter distributions that were obtained by geometrical evaluation (i.e., measuring the diameter of randomly selected ligaments at their center).

Results and Discussion

Bimetallic np-Au

160 The catalytic results for CO and methanol oxidation using bimetallic np-Au with different amounts of residual Ag are depicted in Figure 2. The reactant gases CO and O₂ were supplied and varied while keeping a stoichiometric ratio (CO: O₂; 2:1). As deduced from Figure 2 (a), the production of CO₂ continuously increases with increasing supply of reactants. The fact that the conversion does not linearly depend on the supply of reactants points to mass transport limitation as detailed in ref²⁰. The characteristics are exemplarily shown for four different samples prepared by *free* as well as *galvanic corrosion* and containing different amounts of residual silver between ~ 0.5 at% and 11 at% (as determined by AAS). All measurements were performed directly after activating²⁰ the particular sample to exclude any variation of activity due to, for example, a possible deactivation over time. Comparing the activities, it is obvious that the total activity for the sample containing 11 at% Ag is about two times higher than the activities of the other samples with Ag concentrations between 0.5 and 1.2 at%. As the concentration of Ag within the bulk and the concentration of Ag on the surface –
170 the latter being decisive for the catalytic behaviour, of course - are related but not equal²⁰, one has to be careful when drawing conclusions based on the Ag bulk content. The trend, however, is clear and underlines that the catalytic activity of np-Au for CO oxidation greatly benefits from high residual Ag concentrations and can be enhanced by about 100 % when changing the Ag content from ~1 at% to 11 at%.

The results for the oxidation of methanol in the temperature regime between 20 °C and 80 °C are depicted in Figure 2 (b). Starting at 20 °C, partial oxidation is observed leading to methyl formate as the only product.³³ The unfavourable total oxidation to CO₂ is largely suppressed. When the temperature is raised, the conversion of methanol increases considerably. A different picture emerges when using np-Au samples containing higher amounts of residual Ag. For example, when
180 using a sample containing 2.5 at% residual Ag, the total oxidation becomes more pronounced and the selectivity (fraction of methyl formate) decreases to about 85 %. In case of samples very rich in Ag (~ 10 at%) no formation of methyl formate takes place at all. In this case only the total oxidation product CO₂ can be observed. Generally, the activity (sum of all products) tends to decrease with an increase of Ag. Thus, in contrast to CO, in case of methanol increasing concentrations of Ag are unfavourable leading to more pronounced total oxidation and a decrease of total activity.



190 **Figure 2 : Catalysis with np-Au: influence of Ag on the activity and selectivity for two different reactions. (a) Conversion of CO to CO₂ using np-Au samples containing different amounts of Ag (at 40 °C). (b) The oxidation of methanol with molecular oxygen (2 vol% methanol + 1 vol% O₂) in the temperature regime between 20°C and 80°C. Only two products are formed, methyl formate (grey squares) and the total oxidation product CO₂ (blue diamonds). In the inset, the selectivity (in percent) for the favoured partial oxidation product methyl formate is shown as a function of the Ag content of np-Au (2 vol% methanol + 1 vol% O₂ at 80 °C). (c) SEM from the middle of the cross section of differently prepared np-Au disks containing different amounts of residual Ag (from left to right 0.5 at%, 2.5 at%, and 10 at%).**

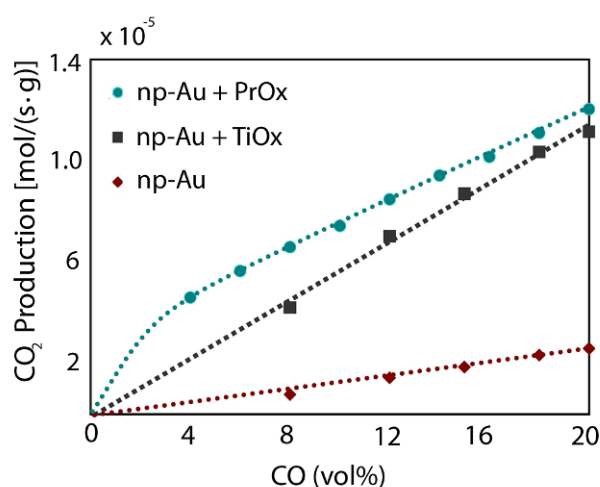
200 *Oxide modification of nanoporous gold*

Most of the highly active gold catalysts studied in the past were comprised of small Au nanoparticles supported on a porous metal oxide, such as titania or ceria.^{15, 34} Besides the advantage of a high dispersion of nanoparticles, the support was also found to be crucial for catalytic activity¹³, as pure gold lacks high activity towards dissociation of molecular oxygen.³⁵ In addition to discussions about the role of low coordinated gold atoms in the literature^{17, 18}, it was speculated whether the support is involved in supplying oxygen for example at the particle perimeter.^{13, 14} Recently, titania was also deployed as a dopant in case of a nanoparticle catalyst to enhance the catalytic activity for CO oxidation.³⁶ As the np-Au provides a self-supporting porous structure, it is especially tempting to modify this structure by a suitable metal oxide, such as titania or praseodymia, in order to achieve enhanced catalytic activity for oxidation reactions, involving molecular oxygen. In a way, this system constitutes an inverse porous metal oxide/metal catalyst.

210

The corresponding results for bare and metal-oxide doped np-Au for CO oxidation are depicted in Figure 3. In all cases, the conversion of CO increases with increasing supply of CO. In these experiments the oxygen partial pressure was kept constant at high excess (> 20 vol%) so that the conversion increases linearly with CO indicating a first order reaction as was also observed in previous studies.²⁰ Notably, the samples modified by either titania or praseodymia deposition show an activity which is enhanced by nearly one order of magnitude. (Note that this comparison is only qualitative and – because of the influence of mass transport - does not directly reflect the differences in the rate of catalytic surface reaction.)

220 In order to exclude any influence from the preparation (e.g. by ethanol applied together with the oxide nanoparticles or the precursors, respectively), samples were also measured after being treated with pure ethanol. For this purpose, one disk of np-Au was broken into 3 pieces. One piece was left as a reference, while another one was treated with a suspension of titania particles and yet another one with pure ethanol. In all cases, an enhanced activity for CO oxidation was *only* observed in case of the titania particles or praseodymia precursor containing suspension. A contribution arising from the treatment of samples with ethanol can thus be excluded.



230 **Figure 3: Activity of pristine np-Au in comparison to PrOx and TiO₂ modified np-Au samples at 60 °C (+ excess of oxygen, i.e. > 20 vol% O₂).**

Measurements with energy dispersive x-ray absorption (EDX) carried out to quantify the amount of material deposited inside the np-Au material revealed no elements apart from Au meaning that the titania and praseodymia concentrations were below the detection limit. Considering that this method is not surface sensitive and rather probes the entire volume of a 30-50 nm thick ligament, one can conclude that the coverage must be well below 1 monolayer. (Note that Ag could not be detected in these EDX experiments, either).

240 To gain further insight into the distribution of either titania or praseodymia, np-Au samples were annealed under inert gas atmosphere. Due to the high surface-to-bulk ratio, np-Au is structurally unstable and shows coarsening of the porous structure upon thermal treatment. This coarsening is entirely due to surface self-diffusion of Au atoms on the surface³⁷, leading to an increase of the ligament diameter from the nm regime to the μm regime.²⁹ Previously, it has been observed that adsorbates (see also next section) can hamper this diffusion process and thus stabilize the nanoporous structure.²⁵ Accordingly, it can be assumed that also oxide deposits on the surface - if localized at step edges e.g. which are natural sources of diffusing atoms - should be able to stabilize the structure.

250 The results for the praseodymia coated sample after annealing to 500 °C are depicted in Figure 4. Clearly, the ligaments close to the outer surface (e.g. 10 μm) are indeed stabilized and no coarsening can be observed (average ligament size 40 nm). In the inner sections of the sample, meaning in the middle of a cross section of a 200 μm sample disc, the size distribution was found to be bimodal, indicating that some ligaments are stabilized while others are not (Figure 4 (b)). Based on this finding one can conclude that in case of praseodymia even (sub-) monolayer amounts of deposited material can stabilize the structure during annealing. While this effect is most pronounced close to the outer surface, the deposition techniques applied here (impregnation) results also in small amounts deposited even in deeper sections (100 μm).

In case of titania, no similar stabilization was observed. Already sections close to the outer surface (e.g. $\sim 5 \mu\text{m}$) showed coarsening of the ligaments. We attribute this to the different deposition techniques (impregnation vs. deposition of nanoparticles). In case of the titania, the particles cannot penetrate so deeply, resulting in a significantly larger gradient.

260 The fact that in *both* cases - TiO_2 and PrO_x modification - an enhanced activity for CO oxidation was detected points towards a contribution of the particular oxide in the catalytic cycle. A scenario similar to supported Au nanoparticles is possible where the oxide contributes to the supply of active oxygen at the perimeter between the oxide and Au.¹³ The increased activity for CO oxidation is presumably linked to an enhanced activation of molecular oxygen. (Please note that neither of the oxides is catalytically active for the CO oxidation at temperatures below 200 °C.^{38, 39}) Interestingly, the samples treated with a titania particle suspension show an increased activity for CO oxidation in the same order as praseodymia, revealing that a simple treatment with nanoparticles - leading to a high coverage with oxide within a thin layer - can be as effective as a the more extended coverage obtained with impregnation.

270

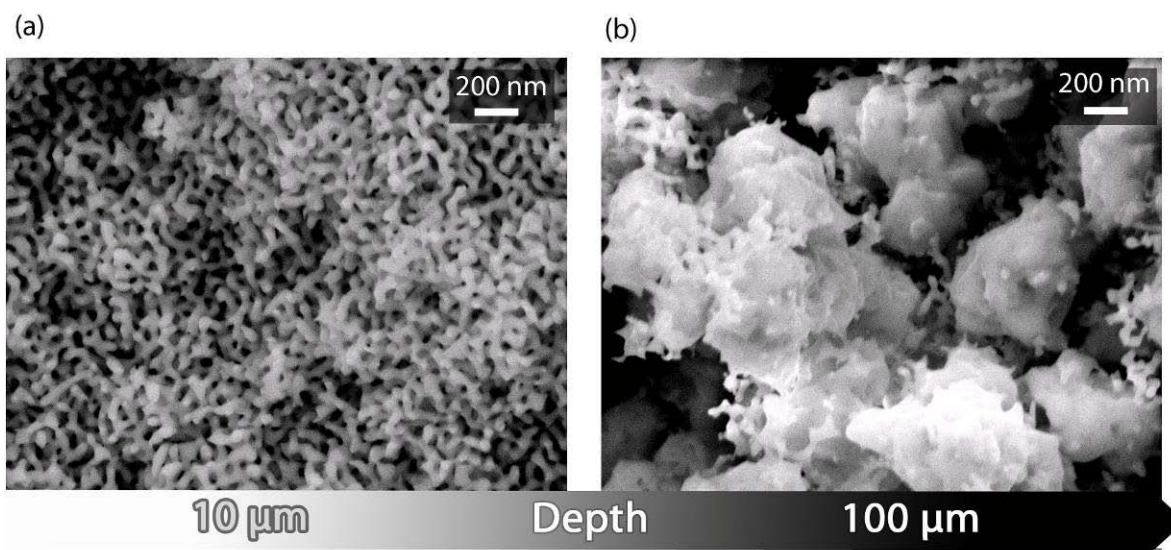


Figure 4: Cross sectional scanning electron micrographs (XSEM) of a praseodymia coated sample after annealing to 500 °C. (a) Areas close to the outer surface (~ 10 - 15 μm) are apparently stabilized, ligament size (~ 40 nm) and morphology are not affected by the heat treatment. (b) Inner sections of the sample (~ 100 μm) clearly reveal a bi-modal ligament size distribution. Some ligaments are still ~ 40 nm in size while other grew to more than 100 nm.

280 *Tailoring structures using adsorbates*

Using nanoporous gold in a monolithic form not only offers advantages (such as increased mechanical and thermal stability as well as good thermal conductivity), but also the disadvantage of more severe mass transport limitation reducing the effectiveness of the catalyst.²⁰ This is due to the pores in the nanometer regime which limit the transport of the reactants into the structure and of the products out of the structure, respectively. This problem becomes even more pronounced, the faster the catalytic reaction proceeds. The increased activity of for example oxide modified np-Au will lead to an even lower efficiency if diffusion of reactants is not enhanced as well. One possibility to optimize mass transport limitation is of course a tailoring of the pore structure by thermally induced coarsening. In the following we will show results obtained by annealing in inert and oxidative gas atmospheres.

290

The resulting averaged ligament diameters obtained after thermal treatment are summarized in Figure 5. When annealing at 450 K in a helium atmosphere, the size of the ligament increase from initially 40 nm to roughly 80 nm after 3 hours. When further increasing the temperature to 650 K, the average ligament diameter increases to more than 500 nm.

This finding is well in line with previous studies on coarsening of np-Au.²⁵ In case of self-diffusion of the Au atoms on the surface – which is presumably the main pathway for thermally induced coarsening at these temperatures - one would expect an Arrhenius type temperature dependency.^{37, 40}

Indeed, the ligaments size as a function of temperature follows an exponential trend and becomes far more pronounced for higher temperatures.

300 In case of annealing under an ozone containing atmosphere, the behaviour is greatly changed though. Below 500 K, where oxygen forms a stable adsorbate layer²⁵, the ligament size apparently does not increase. The origin for this adsorbate induced stabilization can be understood in terms of an increased activation barrier for oxygen bonded Au atoms when “jumping” between surface sites, which is the precondition for surface self-diffusion.³⁷ At temperatures higher than 500 K, however, the residence time of atomic oxygen on Au is drastically reduced from about 1 second at 530 K to only milliseconds at 650 K (assuming first order desorption kinetics).^{35, 41} Accordingly, the coverage of the surface with atomic oxygen becomes too small to stabilize the structures furthermore. At temperature of 570 K and 650 K the results for the samples exposed to ozone or an inert gas atmosphere are almost indistinguishable, indicating that the coverage of oxygen is negligibly small at these temperatures.

310

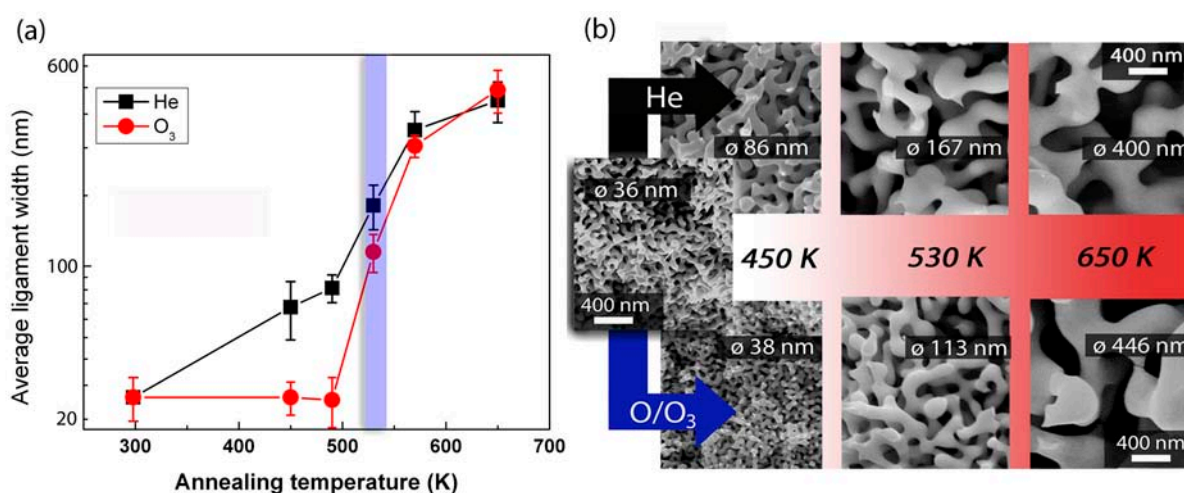


Figure 5: (a) The run of the average ligament diameter after annealing of np-Au under O₃ containing (~ 7 vol%) and inert gas (He) atmospheres for 3 hours (only ligaments close to the outer surface were included in the evaluation). Below the desorption temperature of atomic oxygen on gold (~ 530 K) its surface coverage is high enough to prevent coarsening of the nanoporous structure. (b) Corresponding XSEM from the cross section of a np-Au disk after annealing to the particular temperature for 3 hrs. All images are scaled to the same magnification.

320 All results discussed so far do not consider mass transport phenomena and are thus only applicable to regions close to the outer surface of the np-Au material. Interestingly, when investigating the cross section of thick np-Au samples (> 200 μm), gradients in the ligament and pore size distribution are obvious (see Figure 6). After annealing at 450 K under ozone containing atmosphere, the structure close to the outer surface is obviously stabilized, as discussed above. On the contrary, the inner sections of the sample exhibit larger structures (ligament diameters > 100 nm) as one would

330 expect for a sample annealed under an inert gas atmosphere. Obviously, the supply of ozone from the outer gas phase is restricted by mass transport through the pores of the material. These characteristics can be described semi-quantitatively, employing a simple kinetic model. The coverage of the surface by oxygen is a function of the impingement rate (ozone molecules hitting the surface per unit of time), the sticking coefficient (probability of a hit leading to O_{ads}), and the desorption rate (oxygen atoms desorbing from the surface per unit of time). The impingement rate of ozone molecules on the surface of a particular ligament is obviously a function of depth. The net impingement rate J_{CF} can be described by the impingement rate on a flat surface J rectified by the transmission factor (molecules only hitting the outer surface are repelled) and a factor CF (Clausing factor)⁴² which takes into account the aspect ratio of the particular pores:

$$J_{CF} = \Lambda \cdot J \cdot CF = \Lambda \cdot \frac{N_a \cdot P}{\sqrt{2\pi \cdot M \cdot R \cdot T}} \cdot \frac{1}{1 + \frac{3\lambda}{4d}},$$

340 where N_a is the Avogadro constant, P the (partial-) pressure in the ambient gas phase, M is the molecular mass, R the universal gas constant, T the temperature, λ the pore length and d the pore diameter. In this way, the supply of ozone by the outer gas phase can be described as a function of depth. The resulting coverage of the surface with atomic oxygen at 450 K as a function of distance from the outer gas phase is shown in Figure 6 (b) (assuming first order desorption rate of atomic oxygen^{25, 35}, a sticking coefficient of 0.01⁴³, and a transmission factor of 0.7 corresponding to about 70 % void volume of the material). The supply of ozone close to the outer surface generates roughly one monolayer of oxygen which is the upper limit observed in experimental studies.⁴⁴ However, after about 5 μm distance from the outer sample surface, the O coverage of the surface strongly decreases. At a depth of around 50 μm , the surface coverage accounts for only about one tenth of a monolayer. Since only beyond this depth an increase of the ligament diameter is observed, one can conclude that not only a full oxygen monolayer but also submonolayers (above $\theta \sim 0.1$) lead to a stabilization of the ligaments. This finding is in line with a kinetic model of surface diffusion based dealloying.^{2, 5} Atoms at or close to step edges are most unstable and thus prone to diffusion. Presumably, the stabilization of step edges and low coordinated atoms by atomic oxygen is crucial for the stabilization of structures during annealing.

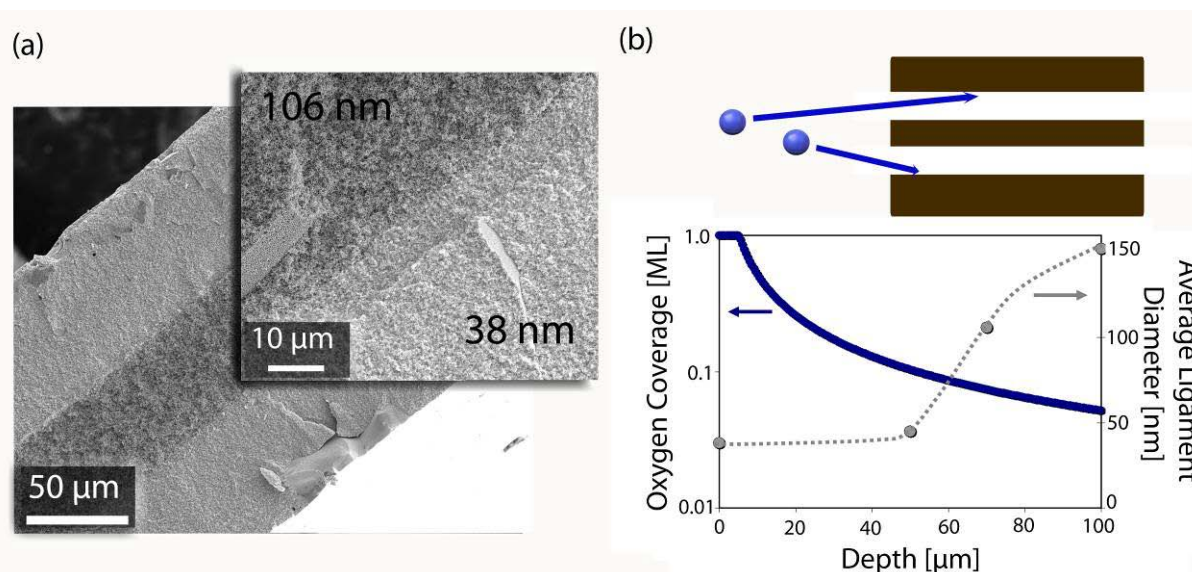


Figure 6: Structural tuning of np-Au based on surface chemistry. (a) Scanning electron micrographs of a cross section of a np-Au disk after annealing at 450 K for 3 hrs under an ozone containing oxygen atmosphere (~ 7 vol%). The regions close to the outer surface are obviously stabilized by adsorbed atomic oxygen while the ligaments in the inner section of the disk show coarsening. (b) Development of the (averaged) ligament diameter as a function of distance (depth) from the outer surface. In the lower section a semi-quantitative description of the oxygen surface coverage at 450 K and the ligament size across a np-Au disk after annealing to 450 K are shown.

360

Conclusions

Three different methods of controlled modification of the properties of np-Au were employed with the emphasis on catalysis. As np-Au exhibits a well reproducible and self-supporting porous nanostructure without the need of a support, it is particularly suitable for structural and chemical modifications. For example, by variation of dealloying conditions, one can vary the content of Ag remaining in the material after preparation from 0.5 at% to even more than 10 at%. As the Ag content controls the availability of surface oxygen, total oxidation reactions, such as the oxidation of CO, greatly profit from an increased Ag content. This finding is well in line with reports from bimetallic supported Au-Ag particles.¹⁹ Partial oxidation reactions, such as the oxidation of methanol, however, benefit from lower concentrations of Ag. It is thus important to tailor the amount of residual Ag for a specific catalytic application. (Using the dealloying route to prepare different bimetallic catalysts, one is limited to concentrations in the order of 10-15 at%. The reason is that a certain amount of Ag has to be dissolved in order to achieve homogeneous porosity.)

370

Furthermore, we employed post-dealloying modification by adding metal-oxides to the porous structure of np-Au. In a first attempt, two different metal-oxides were chosen. Titania (TiO₂) is a commonly used support material for gold based catalysts, which itself is very unreactive towards oxidation of CO³⁹. Additionally, we chose praseodymia, a less often used metal-oxide in catalysis. In the group of rare earth oxides, which includes also for example ceria, it is the one with the highest oxygen mobility, which, however, is only active for CO oxidation at temperatures starting around

380

300 °C.³⁸ We observe a strongly enhanced catalytic activity for CO oxidation at temperature below 100 °C for both oxides, pointing to a strong synergistic effect. The different preparation conditions and the involved mass transport limitations yet prevent a straightforward comparison of activities between both metal-oxide modified systems.

To reduce mass transport limitations without destruction of the monolithic and porous structure a tailored design of the ligament and pore sizes is mandatory. We show that, by using thermally induced coarsening under the influence of adsorbates, one can not only increase the pore diameter but also induce gradients in the pore size distribution along the cross section of a sample. This opens the door for introducing a bimodal and hierarchical pore and ligament size distribution and thus an optimized mass transport.

Acknowledgements

We thank the University Bremen for financial support. Work at LLNL was performed under the auspices of the U.S. DOE by LLNL under Contract DE-AC52-07NA27344. We gratefully acknowledge the experimental support (SEM) of Petra Witte (Prof. Willems, Historical Geology – Palaeontology, Geology department of the University Bremen).

References

1. J. Lee, O. K. Farha, J. Roberts, K. A. Scheidt, S. T. Nguyen and J. T. Hupp, *Chem. Soc. Rev.*, 2009, **38**, 1450-1459.
2. J. Erlebacher and R. Seshadri, *MRS Bull.*, 2009, **34**, 561-568.
3. J. S. King, A. Wittstock, J. Biener, S. O. Kucheyev, Y. M. Wang, T. F. Baumann, S. K. Giri, A. V. Hamza, M. Bäumer and S. F. Bent, *Nano Lett.*, 2008, **8**, 2405-2409.
4. J. Biener, A. Wittstock, T. Baumann, J. Weissmüller, M. Bäumer and A. Hamza, *Materials*, 2009, **2**, 2404-2428.
5. J. Erlebacher, M. J. Aziz, A. Karma, N. Dimitrov and K. Sieradzki, *Nature*, 2001, **410**, 450-453.
6. A. J. Forty, *Nature*, 1979, **282**, 597-598.
7. J. Erlebacher, *J. Electrochem. Soc.*, 2004, **151**, C614-C626.
8. R. C. Newman, S. G. Corcoran, J. Erlebacher, M. J. Aziz and K. Sieradzki, *MRS Bull.*, 1999, **24**, 24-28.
9. J. Biener, A. Wittstock, L. A. Zepeda-Ruiz, M. M. Biener, V. Zielasek, D. Kramer, R. N. Viswanath, J. Weissmuller, M. Bäumer and A. V. Hamza, *Nat. Mater.*, 2009, **8**, 47-51.
10. V. Zielasek, B. Jürgens, C. Schulz, J. Biener, M. M. Biener, A. V. Hamza and M. Bäumer, *Angew. Chem.-Int. Edit.*, 2006, **45**, 8241-8244.
11. C. X. Xu, J. X. Su, X. H. Xu, P. P. Liu, H. J. Zhao, F. Tian and Y. Ding, *J. Am. Chem. Soc.*, 2007, **129**, 42-43.
12. M. Haruta, T. Kobayashi, H. Sano and N. Yamada, *Chemistry Letters*, 1987, 405-408.
13. G. C. Bond and D. T. Thompson, *Gold Bull.*, 2000, **33**, 41-51.
14. G. C. Bond and D. T. Thompson, *Catalysis Reviews-Science and Engineering*, 1999, **41**, 319-388.

15. A. S. K. Hashmi and G. J. Hutchings, *Angew. Chem.-Int. Edit.*, 2006, **45**, 7896-7936.
16. Y. Ding and M. W. Chen, *MRS Bull.*, 2009, **34**, 569-576.
17. H. Falsig, B. Hvolbaek, I. S. Kristensen, T. Jiang, T. Bligaard, C. H. Christensen and J. K. Norskov, *Angew. Chem.-Int. Edit.*, 2008, **47**, 4835-4839.
18. J. K. Norskov, T. Bligaard, B. Hvolbaek, F. Abild-Pedersen, I. Chorkendorff and C. H. Christensen, *Chem. Soc. Rev.*, 2008, **37**, 2163-2171.
19. B. Jürgens, C. Kübel, C. Schulz, T. Nowitzki, V. Zielasek, J. Biener, M. M. Biener, A. V. Hamza and M. Bäumer, *Gold Bull.*, 2007, **40**, 142-149.
- 430 20. A. Wittstock, B. Neumann, A. Schaefer, K. Dumbuya, C. Kübel, M. M. Biener, V. Zielasek, H.-P. Steinrück, J. M. Gottfried, J. Biener, A. Hamza and M. Bäumer, *J. Phys. Chem. C*, 2009, **113**, 5593-5600.
21. C. B. Wang, G. Deo and I. E. Wachs, *J. Phys. Chem. B*, 1999, **103**, 5645-5656.
22. M. Haruta, *ChemPhysChem*, 2007, **8**, 1911-1913.
23. L. V. Moskaleva, S. Rohe, A. Wittstock, V. Zielasek, T. Kluner, K. M. Neyman and M. Bäumer, *Phys. Chem. Chem. Phys.*, 2011.
24. X. B. Ge, X. L. Yan, R. Y. Wang, F. Tian and Y. Ding, *J. Phys. Chem. C*, 2009, **113**, 7379-7384.
- 440 25. J. Biener, A. Wittstock, M. M. Biener, T. Nowitzki, A. V. Hamza and M. Bäumer, *Langmuir*, 2010, **26**, 13736-13740.
26. M. Hakamada and M. Mabuchi, *J. Mater. Res.*, 2009, **24**, 301-304.
27. J. Biener, G. W. Nyce, A. M. Hodge, M. M. Biener, A. V. Hamza and S. A. Maier, *Adv. Mater.*, 2008, **20**, 1211-1217.
28. X. Y. Lang, L. Y. Chen, P. F. Guan, T. Fujita and M. W. Chen, *Appl. Phys. Lett.*, 2009, **94**, 3.
29. A. M. Hodge, J. R. Hayes, J. A. Caro, J. Biener and A. V. Hamza, *Adv. Eng. Mater.*, 2006, **8**, 853-857.
30. J. Biener, M. M. Biener, T. Nowitzki, A. V. Hamza, C. M. Friend, V. Zielasek and M. Bäumer, *ChemPhysChem*, 2006, **7**, 1906-1908.
- 450 31. C. C. Jia, H. M. Yin, H. Y. Ma, R. Y. Wang, X. B. Ge, A. Q. Zhou, X. H. Xu and Y. Ding, *J. Phys. Chem. C*, 2009, **113**, 16138-16143.
32. A. Schaefer, A. Sandell, L. E. Walle, V. Zielasek, M. Schowalter, A. Rosenauer and M. Bäumer, *Surf. Sci.*, 2010, **604**, 1287-1293.
33. A. Wittstock, V. Zielasek, J. Biener, C. M. Friend and M. Bäumer, *Science*, 2010, **327**, 319-322.
34. G. J. Hutchings, *Catalysis Today*, 2005, **100**, 55-61.
35. J. M. Gottfried, K. J. Schmidt, S. L. M. Schroeder and K. Christmann, *Surf. Sci.*, 2003, **525**, 184-196.
36. R. Guttel, M. Paul and F. Schüth, *Catalysis Science & Technology*, 2011.
37. G. Antczak and G. Ehrlich, *Surf. Sci. Rep.*, 2007, **62**, 39-61.
- 460 38. Y. Borchert, P. Sonström, M. Wilhelm, H. Borchert and M. Bäumer, *J. Phys. Chem. C*, 2008, **112**, 3054-3063.
39. U. Diebold, *Surface Science Reports*, 2003, **48**, 53-229.
40. A. S. Dalton and E. G. Seebauer, *Surf. Sci.*, 2007, **601**, 728-734.
41. J. M. Gottfried, K. J. Schmidt, S. L. M. Schroeder and K. Christmann, *Surf. Sci.*, 2003, **525**, 197-206.
42. R. G. Gordon, D. Hausmann, E. Kim and J. Shepard, *Chem. Vapor Depos.*, 2003, **9**, 73-78.
43. J. Kirn, E. Samano and B. E. Koel, *Surf. Sci.*, 2006, **600**, 4622-4632.
44. N. Saliba, D. H. Parker and B. E. Koel, *Surf. Sci.*, 1998, **410**, 270-282.